ROYAL SOCIETY OF CHEMISTRY

COMMUNICATION

Check for updates

Optical property control of π-electronic systems bearing Lewis pairs by ion coordination†

Takahiro Yanbe, Kei Mizuguchi, Ryohei Yamakado [ID] * and Shuji Okada [ID]

π-Electronic systems bearing Lewis pairs were synthesized and their optical responses to added ions were investigated. The tuning of the optical properties was demonstrated by the addition of various ion pairs, and these behaviours were elucidated by theoretical calculations.

The development of donor–π–acceptor (D–π–A) molecules, in which an electron-rich donor and an electron-poor acceptor are linked by π-conjugated moieties to enable intramolecular charge transfer (ICT), has attracted much attention because these compounds find various applications, including in fluorescent materials,[1] dye-sensitized solar cells,[2] and second-order nonlinear optics.[3] The optical properties of D–π–A molecules with a large dipole moment can be controlled by the solvent polarity. However, the effective control of these properties in the solid state remains unexplored. In order to modify the optical properties of D–π–A molecules by changing their surroundings in the solid state, thermally stable components such as ion pairs are required. Anion and cation receptors are sensitive to ions and form complexes with such species.[4,5] Hence, π-electronic systems containing both cation and anion receptors would display multi-responsive properties to ion pairs. However, such ion-pair receptors have been rarely studied.[6]

As ion pair receptors, we focused on Lewis pairs (LPs). The potential use of boron compounds, a Lewis acid, to detect anions such as F⁻ and CN⁻ has been reported.[7] Although π-electronic systems bearing Lewis pairs have been reported, their ion-binding behaviour has not been studied.[8] In order to use a Lewis pair to prevent the formation of a complex through coordination bonds, it is necessary to introduce bulky substituents. Combinations of Lewis bases (such as trimesitylphosphine) and acids (such as tris(pentafluorophenyl)borane)

bearing bulky substituents are called frustrated Lewis pairs (FLPs). FLPs are used as organic catalysts because of their unique arrangement of Lewis acid and base that enables the activation of relatively inert small molecules such as dihydrogen.[9] Recently, FLPs were employed for fabricating self-healing[10] and CO₂-responsive materials.[11] There are also a few reports on ion-pair coordination by FLPs.[12] Inspired by the properties of FLPs, we hypothesised that the electronic structure of π-electronic systems containing a Lewis pair with bulky substituents can be controlled by adding ion pairs even in the solid state (Fig. 1a), resulting in control over various optical properties using a single π-conjugated molecule. In this study, we investigated the interaction between LPs and ion pairs and revealed the optoelectronic properties of LP-containing π-electronic systems in the presence of different ion pairs.

The designed LP-containing diphenylacetylenes (**1a**, **b**, Fig. 1b) combine one of two kinds of Lewis base, phosphine or amine, and one Lewis acid, borane, and were prepared in high yields by Sonogashira coupling of (4-iodophenyl)dimesitylborane with 4-ethynyl-N,N-diphenylaniline or (4-ethynylphenyl)diphenylphosphine, respectively, in a diisopropylamine/toluene mixture in the presence of CuI and Pd(PPh₃)₄. Compounds **1a** and **1b** were characterised by

Department of Organic Materials Science, Graduate School of Organic Materials Science, Yamagata University, Yonezawa 992-8510, Japan.
E-mail: yamakado@yz.yamagata-u.ac.jp
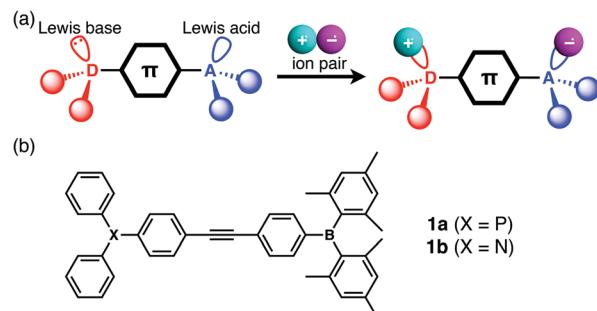
Fig. 1 (a) Schematic illustration of the complex formation between a LP-containing π-electronic system and ion pair, and (c) the chemical structures of **1a** and **1b**.
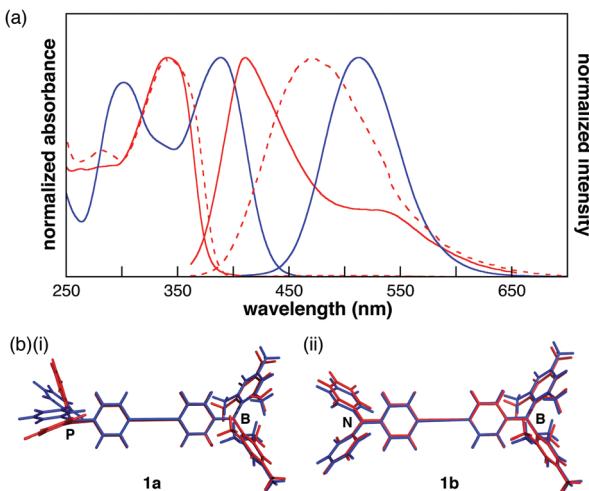
Fig. 2 (a) UV-vis absorption and emission spectra of **1a** (red) and **1b** (blue) in CH_2Cl_2 (10^{-5} M) (solid line) and the film state (dotted line), (b) optimized structures of (i) **1a** and (ii) **1b** at the S_0 (red) and S_1 (blue) states.

NMR, UV-vis spectroscopy, and ESI-MS analyses. The broad ^{11}B NMR signals of **1a** and **1b** at approximately 73 ppm (CH_2Cl_2) were typical of trigonal-planar boron centres. The ^{31}P NMR signal of **1a** at −4.45 ppm was comparable to that of PPh$_3$ (−4.50 ppm, CH_2Cl_2).

In the UV-vis spectra of **1a** and **1b** (10^{-5} M in CH_2Cl_2), the absorption maxima were observed at 342 and 388 nm, respectively (Fig. 2a). The lowest-energy absorption band, which was assigned to the ICT transition by time-dependent density functional theory (TD-DFT) calculations at the B3LYP/6-311+G(d,p)//B3LYP/6-31G(d,p) (PCM = CH_2Cl_2) level of theory,[13] was red-shifted by the replacement of the donor moiety from phosphine to amine. Although **1b** showed a structureless fluorescence spectrum with a peak at 513 nm, **1a** exhibited a fluorescence maximum at 411 nm with a shoulder at 530 nm (Fig. 2a). The lowest-energy fluorescence band of **1a** derived from ICT was red-shifted from that of **1b**, indicating that **1a** undergoes a larger conformational change in its excited state than **1b**. TD-DFT calculations were performed using the optimized structures in the first excited (S_1) state to elucidate the fluorescence spectra. In the optimized structure of **1a**, a large conformational change from the ground state (S_0) to the S_1 state was observed around the phosphine moiety, while the conformation around the borane changed only slightly (Fig. 2b(i)). The HOMO of **1a** in the S_1 state is localized on the phosphorus atom and the two terminal phenyl rings, whereas in the S_0 state it is localized on the phosphorus atom and diphenylacetylene moiety (Fig. S8, ESI†). As such, the higher HOMO level of **1a** in the S_1 state corresponds to the emission in the long wavelength region. In contrast, the optimized structures of **1b** around the nitrogen and borane atoms differ only slightly between the S_0 and S_1 states (Fig. 2b(ii)). Therefore, the HOMO–LUMO energy gap of **1b** in the S_1 state was larger than that of **1a**. Additionally, the absorption maxima of **1a** and **1b** were not influenced by the solvent, whereas the peaks of the fluorescence spectra red-shifted with the increase in the solvent's dielectric constant

(Fig. S4, ESI†). These results suggest a large polarization in the excited states. In the film, the absorption and fluorescence bands of **1a** were observed at 340 and 469 nm, respectively (Fig. 2a). The similarity between the absorption spectra of the film and the CH_2Cl_2 solution indicated that the aggregation of the π-electronic systems was inhibited by the bulky substituents on the boron and phosphorus atoms. On the other hand, in the fluorescence spectrum of **1a** in the film state, the fluorescence band at 411 nm accompanied by a shoulder band was changed to a broad structureless spectrum, which may indicate that the conformational change in the S_1 state was restricted in the film.

The ion-binding properties of **1a** in solution were investigated by ^{11}B and ^{31}P NMR spectroscopy. The ^{11}B NMR signal of **1a** at approximately 73 ppm decreased and a new peak corresponding to **1a**–F$^-$ appeared at 5.04 ppm upon addition of F$^-$ as a TBA salt in CH_2Cl_2 (Fig. 3a). Similarly, the peaks at −0.53 and −13.38 ppm were observed upon addition of AcO$^-$ and CN$^-$, respectively (Fig. 3a and Fig. S12–S14, ESI†). Thus, the bindings of F$^-$, AcO$^-$, and CN$^-$ to the boron centre were demonstrated. Moreover, the sharp high-field-shifted signal of **1a**–CN$^-$ may suggest strong anion binding and restricted pyramidal conformation of a boron centre by the large anion. However, no boron–anion complexes were obtained by the addition of Cl$^-$ and Br$^-$, although tris(pentafluorophenyl)borane gives an anion complex with Cl$^-$ and Br$^-$ (Fig. S11, ESI†). These results indicated that the anion-binding ability is increased by electron-withdrawing groups such as pentafluorophenyl substituents on the boron atom and decreased by bulky and electron-donating groups such as mesityl substituents. Next, complex formation with MCN (M = Ag or Cu) was investigated (Fig. 3b). As AgCN and CuCN are insoluble in CH_2Cl_2, the
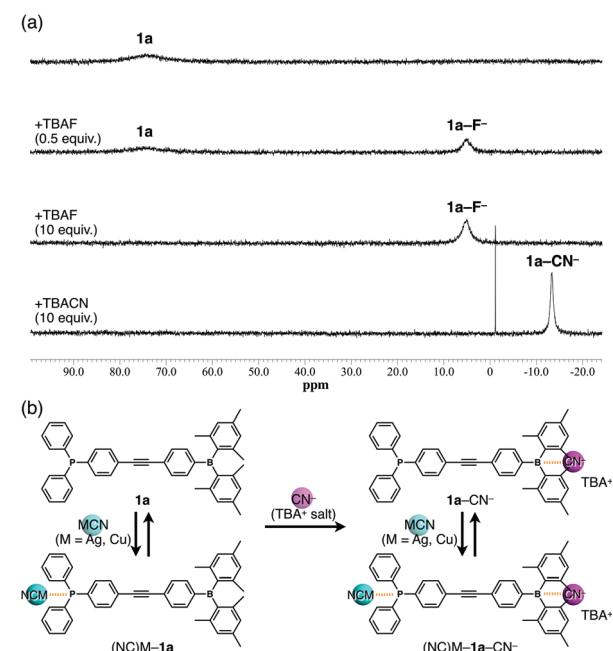
Fig. 3 (a) ^{11}B NMR spectra of **1a** (5.5 mM in CH_2Cl_2) before and after the addition of F$^-$ (0.5 and 10 equiv.) and CN$^-$ (10 equiv.) as TBA$^+$ salts, (b) formation of **1a**–CN$^-$, (NC)M–**1a**, and (NC)M–**1a**–CN$^-$ complexes (M = Ag, Cu).

samples were prepared by heating mixtures of **1a** and 1 equiv. of AgCN or CuCN in CH_2Cl_2 to complete dissolution.[14] The ^{31}P NMR signals of (NC)Ag–**1a** and (NC)Cu–**1a** at 9.62 and −3.59 ppm, respectively, differed from that of **1a** (−5.05 ppm). In contrast, the ^{11}B NMR spectra remained unchanged. These results indicated that CN^- did not act as a free anion, which would undergo complexation with borane, because of the high binding ability of Ag^+ or Cu^+. Therefore, a further 1 equiv. of CN^- was added as TBACN (Fig. 3b), upon which a new ^{11}B NMR signal at −13.27 ppm was observed in both the (NC)Ag–**1a** and (NC)Cu–**1a** samples, indicating the coexistence of free borane and B–CN^- complexes. Moreover, new signals appeared in the ^{31}P NMR spectra between those of the free and coordinated phosphines.‡ Hence, anion-free species (free **1a**) and mono-, and dicoordinated species ((NC)M–**1a** or **1a**–CN^-, and (NC)M–**1a**–CN^-, respectively) coexisted in solution as shown.

The effect of ion-binding in the π-electronic systems was revealed by the UV-vis absorption and fluorescence spectral changes of **1a** and **1b**. Upon addition of F^- as a TBA^+ salt, the absorption maxima of **1a** and **1b** (λ = 342 and 388 nm, respectively) decreased in intensity and shifted to 324 and 348 nm, respectively (Fig. 4a). Similar blue-shifts were also observed upon addition of CN^- and AcO^- as TBA^+ salts, suggesting that the corresponding $\pi \rightarrow p_\pi(B)$ CT transition was quenched by the anion-binding, in which the empty boron p-orbital was filled by the electrons of the anions. The fluorescence spectra of **1a** and **1b** upon the addition of 3 equiv. of anions in CH_2Cl_2, were also measured. Interestingly, although **1b** provided similar spectra by the addition of F^- and CN^-, **1a** provided different spectra depending on the anion complexes (Fig. 4b). In the presence of F^-, the fluorescence at 411 nm with a shoulder at 530 nm of **1a** disappeared, and a new weak and broad fluorescence band at 483 nm appeared. In contrast, fluorescence of higher intensity was observed at 461 nm in the presence of CN^-. The quantum yields for **1a**, **1a**–F^-, and **1a**–CN^- were 6, 27, and 18%, respectively. The spectral changes upon anion addition can be explained by the TD-DFT calculations. In **1a**–F^- and **1a**–CN^-, the absorption band at the long wavelength region corresponds to the ICT from the phenyl attached to the borane–anion complex to the phenyl substituted with the phosphine, whereas that of **1a** stemmed from the ICT in the opposite direction (from the phenylphosphine toward the phenylborane, Fig. 4b(i)). Therefore, the borane–anion complex behaves as a donor. In addition, the electron density of the anion affects the HOMO level, especially in the S_1 state, clarifying the difference between the fluorescence spectra of **1a**–F^- and **1a**–CN^-. Moreover, the larger oscillator strength of **1a**–CN^- (f = 1.260) than of **1a** (f = 0.106) and **1a**–F^- (f = 0.791) was consistent with the experimental fluorescence intensity. However, the HOMO of **1b**, **1b**–F^-, and **1b**–CN^- is localized on the aniline moiety, whereas the LUMO is localized on the ethynyl moiety (Fig. 4b(ii)). Consequently, the anion complexes of **1b** provided similar fluorescence spectra regardless of the anions.

The control over the optical properties of **1a** by the addition of ion pairs was demonstrated in film samples. Spin-coated films of **1a**, **1a**–F^-, **1a**–CN^-, (NC)Ag–**1a**, (NC)Cu–**1a**, (NC)Ag–**1a**–CN^-,
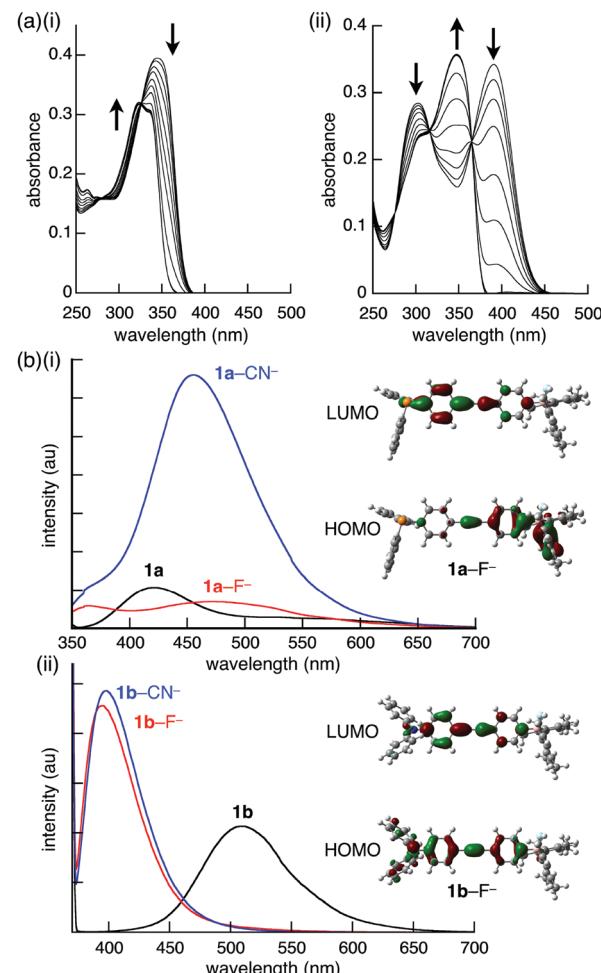
Fig. 4 (a) Changes in the UV-vis absorption spectra of (i) **1a** and (ii) **1b** upon addition of F^- as a TBA^+ salt (10^{-5} M in CH_2Cl_2), (b) emission spectra of (i) **1a** and (ii) **1b** before (black line) and after the addition of 3 equiv. of F^- and CN^- as TBA^+ salts (red and blue lines, respectively; 10^{-5} M in CH_2Cl_2), with the HOMO and LUMO of the S_1 state of the F^- complex calculated by TD-DFT at the B3LYP/6-311+G(d,p)//B3LYP/6-31G(d,p) (PCM = CH_2Cl_2) level.

and (NC)Cu–**1a**–CN^- were prepared from the CH_2Cl_2 solutions of **1a** and its mixtures with 1 equiv. of one or two ion pairs. In the presence of anions, the fluorescence was blue-shifted from that of **1a** (λ = 469, 431, and 461 nm for **1a**, **1a**–F^-, and **1a**–CN^-, respectively), and **1a**–F^- and **1a**–CN^- films exhibited different colours than the corresponding solutions (Fig. 5a). Furthermore, the addition of AgCN (λ = 445) and CuCN (λ = 496) induced blue- and red-shifts, respectively (Fig. 5a). The fluorescence colours of (NC)Ag–**1a** and (NC)Cu–**1a** further changed upon addition of CN^- as a TBA^+ salt as a result of coordination of **1a** by both MCN (M = Ag or Cu) and CN^- in the film. The emission colour coordinates of the film samples on the Commission Internationale de L'Eclairage (CIE) 1931 chromaticity diagram are shown in Fig. 5b. The colours with the CIE coordinates (0.186, 0.255), (0.202, 0.224), (0.212, 0.203), (0.158, 0.130), (0.243, 0.389), (0.197, 0.218), and (0.299, 0.346) were displayed by **1a**, **1a**–F^-, **1a**–CN^-, (NC)Ag–**1a**, (NC)Cu–**1a**, (NC)Ag–**1a**–CN^-, and (NC)Cu–**1a**–CN^-, respectively. Thus, LP-containing
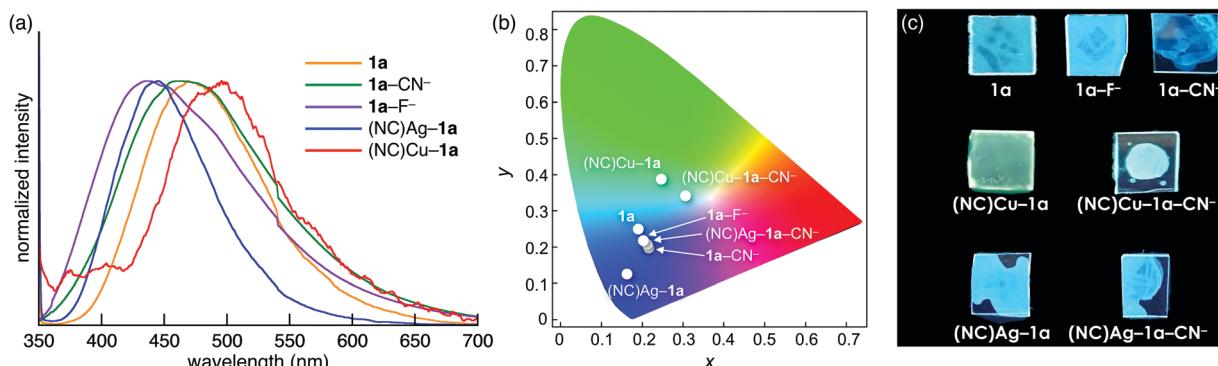
Fig. 5 (a) Changes in the emission spectra, (b) emission colour coordinates in the CIE 1931 chromaticity diagram, and (c) photographs under UV irradiation of **1a** and its complexes with various ion pairs in the film state.

1a is a potential on-demand fluorescent material in the presence of various ion pairs (Fig. 5c).

In summary, LP-containing diphenylacetylenes were synthesized by coupling reactions. The anion-binding properties and the formation of boron–anion complexes were revealed by ^{11}B NMR and UV-vis absorption spectra. High binding constants with F$^-$ and CN$^-$ were obtained. Based on the solution behaviour and the results of the theoretical studies, the electron density provided by coordination with anions led to changes in the energy of the HOMO at the S_1 state, resulting in the fluorescence spectral changes depending on the nature of the anion. Similarly, the phosphorus–metal interaction upon complexation with AgCN and CuCN was observed by ^{31}P NMR spectroscopy. The addition of further CN$^-$ as a TBA$^+$ salt provided the dual complexes. Based on this behaviour, the optical properties of the film samples were controlled by the addition of various ion pairs, and fluorescence colour changes from blue to green were achieved by the combination of one π-electronic system with various ion pairs. Thus, the optical properties of LP-containing diphenylacetylenes in the solid state were controlled by the guest ion pairs. Other ion-pairing combinations for a wider range of spectral changes and different amounts of guest ion pairs are currently under investigation within the development of novel on-demand fluorescent materials.

Conflicts of interest

There are no conflicts to declare.

Notes and references

‡ Although the free borane and its CN$^-$ complex were distinguishable by the ^{11}B NMR, the free and coordinated phosphines were indistinguishable by ^{31}P NMR because of the different time scales of the measurements and the dynamic equilibria.

1 Z. M. Hudson and S. Wang, *Acc. Chem. Res.*, 2009, **42**, 1584–1596.
2 (*a*) Y. Wu and W. Zhu, *Chem. Soc. Rev.*, 2013, **42**, 2039–2058; (*b*) F. Wurthner, *Acc. Chem. Res.*, 2016, **49**, 868–876.
3 (*a*) T. Verbiest, S. Houbrechts, M. Kauranen, K. Clays and A. Persoons, *J. Mater. Chem.*, 1997, **7**, 2175–2189; (*b*) L. Beverina and G. A. Pagani, *Acc. Chem. Res.*, 2014, **47**, 319–329.
4 (*a*) J. L. Sessler, P. A. Gale and W.-S. Cho, *Anion Receptor Chemistry*, RSC Publishing, Cambridge, UK, 2006; (*b*) *Heterocyclic Chemistry*, ed. P. A. Gale and W. Dehaen, Springer-Verlag, Berlin, 2010, vol. 24, pp. 1–370; (*c*) N. Busschaert, C. Caltagirone, W. Van Rossom and P. A. Gale, *Chem. Rev.*, 2015, **115**, 8038–8155.
5 G. W. Gokel, *Comprehensive Supramolecular Chemistry*, ed. J.-M. Lehn, J. L. Atwood, J. E. D. Davies, D. D. MacNicol and F. Vögtle, Pergamon, Oxford, UK, 1996, vol. 1.
6 Y. H. Lee, N. V. Nghia, M. J. Go, J. Lee, S. U. Lee and M. H. Lee, *Organometallics*, 2014, **33**, 753–762.
7 H. Zhao, L. A. Leamer and F. P. Gabbai, *Dalton Trans.*, 2013, **42**, 8164–8178.
8 A. Fukazawa, H. Yamada and S. Yamaguchi, *Angew. Chem., Int. Ed.*, 2008, **47**, 5582–5585.
9 (*a*) G. C. Welch and D. W. Stephan, *J. Am. Chem. Soc.*, 2007, **129**, 1880–1881; (*b*) R. C. Neu, E. Y. Ouyang, S. J. Geier, X. Zhao, A. Ramos and D. W. Stephan, *Dalton Trans.*, 2010, **39**, 4285–4294; (*c*) A. J. Marwitz, J. L. Dutton, L. G. Mercier and W. E. Piers, *J. Am. Chem. Soc.*, 2011, **133**, 10026–10029; (*d*) M. Lindqvist, K. Axenov, M. Nieger, M. Raisanen, M. Leskela and T. Repo, *Chem. – Eur. J.*, 2013, **19**, 10412–10418.
10 (*a*) M. Wang, F. Nudelman, R. R. Matthes and M. P. Shaver, *J. Am. Chem. Soc.*, 2017, **139**, 14232–14236; (*b*) U. Yolsal, M. Wang, J. R. Royer and M. P. Shaver, *Macromolecules*, 2019, **52**, 3417–3425.
11 (*a*) L. Chen, R. Liu and Q. Yan, *Angew. Chem., Int. Ed.*, 2018, **57**, 9336–9340; (*b*) R. Liu, X. Liu, K. Ouyang and Q. Yan, *ACS Macro Lett.*, 2019, **8**, 200–204.
12 (*a*) C. Appelt, J. C. Slootweg, K. Lammertsma and W. Uhl, *Angew. Chem., Int. Ed.*, 2012, **51**, 5911–5914; (*b*) W. Uhl, M. Lange, A. Hepp and M. Layh, *Z. Anorg. Allg. Chem.*, 2018, **644**, 1469–1479.
13 M. J. Frisch, *et al.*, *Gaussian 16 (Revision A.03)*, Gaussian, Inc., Wallingford CT, 2016.
14 Y. Y. Lin, S. W. Lai, C. M. Che, W. F. Fu, Z. Y. Zhou and N. Zhu, *Inorg. Chem.*, 2005, **44**, 1511–1524.